Architectures and protocols for mobile computing applications: a reconfigurable approach

Carla-Fabiana Chiasserini [a], Francesca Cuomo [b,*], Leonardo Piacentini [c], Michele Rossi [d], Ilenia Tinirello [e], Francesco Vacirca [b]

[a] *Polytechnic of Torino, Corso Duca degli Abruzzi 24, 10129 Torino, Italy*
[b] *Dip. INFOCOM, University of Roma "La Sapienza", Via Eudossiana 18, 00184 Roma, Italy*
[c] *University of Perugia, Via G. Duranti 93, 06125 Perugia, Italy*
[d] *University of Ferrara, Via Saragat 1, 44100 Ferrara, Italy*
[e] *University of Palermo, Viale delle Scienze, 90128 Palermo, Italy*

Abstract

This work deals with reconfigurable control functions and protocols for supporting mobile computing applications in heterogeneous wireless systems like cellular networks and WLANs. The control functions are implemented in a software module, named *Reconfigurable Access module for MObile computiNg applications* (RAMON), placed in mobile and/or base stations. RAMON operates on abstract models of the main communication functions of a wireless systems (e.g., transmission over the radio channel, coding end error recovery, capacity sharing and packet scheduling, handover, congestion control, etc.). RAMON algorithms are programmed with reference to the abstract models, independently of specific radio and network technologies. RAMON interactions with a specific wireless access system are conceptually defined by means of parameters that can be measured and controlled, so that the general logic of the module can be posed on top of each system within the constraints and the flexibility provided by the system itself. The implementation of this architectural paradigm requires the definition of specific software *adaptation modules* between RAMON and each specific system. The reconfigurability of RAMON is exploited to adapt and select the algorithms on the basis of user/application requirements. The paper describes the RAMON architectural model and its control algorithms. Specific examples of adaptation modules are also provided. A selection of performance results achieved by a simulator implementing the RAMON module, the adaptation modules and the main communication functions of UMTS, 802.11 and Bluetooth are shown.
© 2003 Elsevier B.V. All rights reserved.

Keywords: Reconfigurable systems; Mobile computing; Resource control; Mobility management; Session control

1. Introduction

In this paper we deal with the design of *Reconfigurable Access module for MObile computiNg applications* (RAMON) and we discuss some results derived from the feasibility study which was

* Corresponding author. Tel.: +39-6-44585640; fax: +39-6-48906114.

E-mail address: cuomo@infocom.ing.uniroma1.it (F. Cuomo).

carried out in an Italian research program, [1] with the participation of six academic research groups. Results of this project have been also presented in [1–4].

RAMON is designed for mobile users demanding TCP/IP services (*mobile computing*). Users can move amongst different wireless networks (named in the following *Reference Environments*, REs). In our feasibility study we consider two different kinds of RE: public cellular systems (e.g., UMTS) and wireless local area systems (e.g., IEEE 802.11, Bluetooth). RAMON aims at supporting (i) *session continuity* when moving in different REs; (ii) *user address portability*, while changing RE; (iii) *transport* Quality of Service (QoS) *performance differentiation*; (iv) *efficient radio resource control*, e.g., different scheduling policies and dynamic capacity sharing; (v) *data integrity* by using adaptive FEC/ARQ techniques; (vi) *energy optimization*, for energy saving at the mobile devices.

RAMON operates at the control plane level and supervises all main architectural layers involved in a communication by managing some key parameters. The joint management of the RE parameters allows for the optimization of the communication process when a mobile user communicates by means of different wireless technologies.

The paper is organized as follows: In Section 2 we review the most relevant articles on reconfigurability that have appeared in the literature, as well as some international projects focusing on this topic. In Section 3 we describe the RAMON functional architecture. Section 4 identifies the *Control Parameters* to provide reconfigurability. Section 5 gives a brief overview of the RAMON algorithms. In Section 6 we describe the architecture of our simulation platform; performance results are discussed in Section 7. Finally, Section 8 draws our main conclusions.

2. Related work

Currently, several on-going research projects deal with the problem of reconfigurability and adaptability [5–8], in order to exploit different wireless access technologies and to offer adaptive and flexible services to mobile users. Reconfigurability is a general concept that can be applied at various protocol stack levels. It includes the development of new programmable transceivers (e.g., FPGA solutions for platform independent physical layers [9–11]), as well as the dynamic adaptation of application, transport and link layers to different transmission scenarios and the definition of algorithms and protocols for providing mobility management and signaling (e.g., Mobile IP dynamic addressing) across inter-technology and inter-operator domains. A discussion on the key functionalities that are required in wireless network technologies in order to support reconfigurability can be found in [12]. The requirements of a reconfigurable multi-standard radio terminal from the physical-layer point of view are highlighted in [13]. In particular, the authors consider a heterogeneous scenario where a multi-standard terminal can access a Bluetooth network, a WLAN and a UMTS network.

The common purposes of the proposed solutions are the integration of various existing systems and performance optimization; however, they differ in terms of architectural choices and primary objectives.

In [14], the authors present an application-specific hardware/software reconfigurable architecture to support adaptive image compression algorithms. The architecture that they propose aims at performance and power efficient implementation, as well as fast and efficient run-time adaptation of an adaptive image compression algorithm.

In [8] an architecture which enables seamless roaming in overlay networks is presented. In particular the project focuses on Mobile IP extensions able to provide simultaneous connectivity over multiple independent wireless networks and to drive interface selection. Heterogeneous systems integration is obtained through a gateway-centric approach: gateway nodes mediate between mobile hosts and each available network. Similar choices

are presented in [7], where the combination of 3G and WLAN wireless technologies is obtained for multi-modal mobile devices through the introduction of a WLAN integration gateway and of a specific software module, on the client side, able to select the best access network. Conversely, in [6] integration is obtained by introducing a basic access network which provides signaling, system discovery and location management for all other wireless systems, and a dedicated radio system on the multi-modal terminal to communicate with the basic access network.

From an architectural point of view, our solution is similar to the one presented in [8] (as it exploits Mobile IP) however our solution is mobile-centric: We assume that each network is connected to the Internet, but we assign all adaptation functions to the mobile client. Moreover, on the client side, our module has some affinities with the module described in [7], in which an interface-abstraction layer is defined in order to map system-independent logic to system-dependent functionalities.

From a performance point of view, the importance of dynamic adaptation as a generic solution to heterogeneity and the importance of cross-layer solutions (e.g., to exploit transport-layer infor-

mation to guide link-level retransmission) is discussed in various papers [5,8,15,16]. These works deal with specific adaptation themes and solve them as separate issues. Our main contribution in this direction is the design of an architecture whose reconfigurability capabilities are extremely flexible and new adaptation criteria and algorithms can be easily developed. This result is obtained through the functional abstraction described in the next section.

3. Functional architecture

RAMON allows the deployment of control algorithms independently of the considered RE. Fig. 1 shows the considered architectural model. RAMON is placed on top of the RE layers dedicated to the radio access functions. It includes a *Common Control* plane (CC-plane) and an *Adaptation* plane (A-plane). Below the A-plane, *Native Control* functionalities (NC-plane) for each RE (denoted as NC/RE-*i* for the *i*th RE) are located. A service development RE-independent *Application Programming Interface* (API) is offered to the overlying application layer. CC-plane functions, which are defined independently of the underlying

API: application Programming Interface CC: Common Control
RE: Reference environment RRC: Radio Resource Control
A: Adaptation SC: Session Control
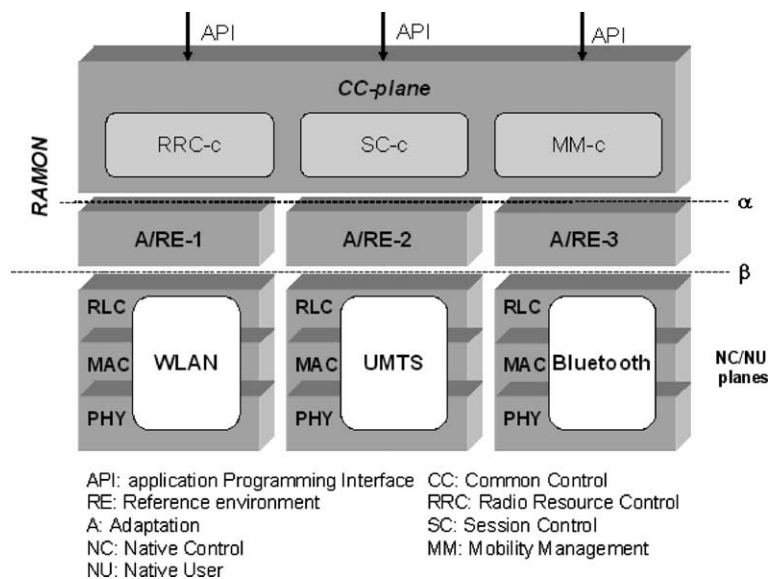NC: Native Control MM: Mobility Management
NU: Native User

Fig. 1. Overall system architecture.

RE, are grouped into three *functional sets*, according to the classical model adopted for wireless communications: (i) *Radio Resource Control* (RRC-c); (ii) *Session Control* (SC-c); (iii) *Mobility Management* (MM-c).

The CC-plane communicates with different REs via the relevant A-planes (A/RE-*i*). CC-plane control functions are exerted by the employment of *RAMON Primitives* (RPs) that allow the exchange of *Control Parameters* (CPs) with the *Native User* plane (NU-plane). Two different types of interfaces can be identified: (i) the α *interface*, between the CC-plane and the A-plane; (ii) the β *interface*, between the A-plane and the NC-plane of each RE. Fig. 2 completes Fig. 1. On the right the CC-plane and the A-plane are depicted, with the relevant α and β interfaces. On the left, the relevant NC-planes and NU-planes are shown, relatively to two generic REs. Fig. 2 shows how the SC-c, MM-c and RRC-c functionalities interact with the corresponding SC-*i*, MM-*i* and RRC-*i* ($i = 1, 2$) of the two REs through the translation performed by the A-planes (A/RE-1, A/RE-2). The relations between the NC-planes and NU-planes are highlighted and particularly how the SC-*i*, MM-*i* and RRC-*i* functionalities are related to *Physical* (PHY-*i*), *Medium Access Control* (MAC-*i*) and *Radio Link Control* (RLC-*i*) functions. Finally, *Applications*, TCP/UDP and IP layers, which are part of the NU-plane, directly interact with the CC-plane.

The RAMON module might be implemented only in the *mobile stations* (MSs), or be included also in the *base station* (BS). In the first case the MS equipped with RAMON is called enhanced MS (eMS) and supports *abstract functionalities* common to all REs. Such functionalities are obtained from the *specific functionalities* of each RE, by means of the A-plane, as previously described. The eMS has at least two radio interfaces implementing the lower layers of the specific radio access technology, e.g., Bluetooth (BT) protocol stack and UMTS. When RAMON is implemented only in the eMS, basic functionalities such as session continuity, mobile controlled handover and logical mobility can be deployed. This scenario might be appealing for mobile users seeking for complete versatility when moving in different radio environments. In other words, a user may migrate (with a single laptop, Personal Digital Assistant, cellular phone) in different REs maintaining seamless communications and QoS performance. Furthermore, it is possible to implement RAMON algorithms also at the BS (named enhanced BS— eBS); the drawback of modifying the BS software might be compensated by the possibility of deploying sophisticated radio resource management schemes aiming at optimizing the overall
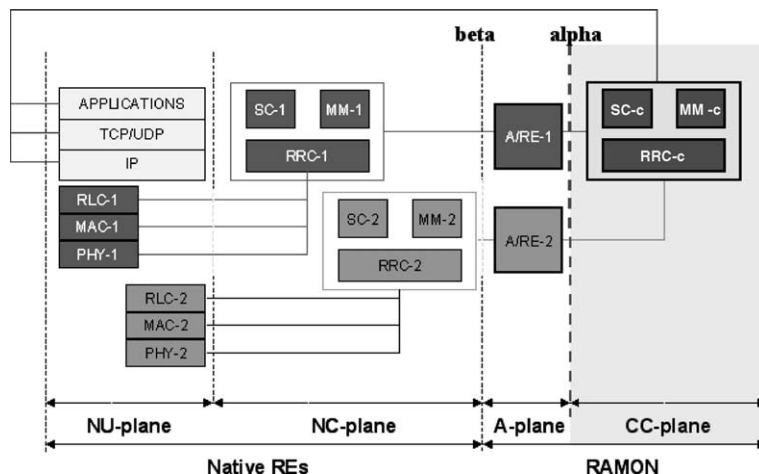

Fig. 2. Basic interactions among control and user planes.

system efficiency. The same BS control software in the CC-plane can be used in different REs thanks to its reconfigurable design.

4. Control parameters

CPs have been introduced to allow the RA-MON module to identify the state of each RE and to configure adequately the overall transmission process, by exploiting the cross-layer paradigm. As a consequence, status information are shared among all layers of the protocol stack. Information sharing may be performed in two directions: (i) *upward sharing*. TCP/IP parameters may be configured to adapt to variable RE characteristics; (ii) *downward sharing*. MAC, RLC and PHY layer parameters can be adapted to transport and application layer requirements. For example, the behavior of the TCP window may be forced to adapt to the time-varying physical channel characteristics (*upward*), while lower layer parameters may be reconfigured, with the aim of serving distinct applications with different QoS requirements

Table 1
Control parameters

Physical layer—PHY	
BAT_LEVEL	Battery level
TX_POWER	Transmitted power
SIR	Signal to interference ratio
Link layer—MAC/RLC	
LINK_PACKET_SIZE	Link layer protocol data unit (PDU) size
BURST_ERR	Average burst error period
ERR_PR	Average protocol data unit error probability
QUEUE_LENGTH	Backlog size
QUEUE_AGE	Age of the oldest packet in the transmission queue
MAX_LINK_RETR	Maximum number of re-transmission attempts per PDU
Transport layer—TCP	
SRTT	Smoothed round trip time
RTO	Retransmission timeout
SSTRESH	Slow start threshold
TRANS_PACKET_SIZE	Average transport layer segment size

(*downward*). Data belonging to NU-planes are passed to the A-planes and then translated into CPs sent to RAMON to be processed by algorithms running in the CC-plane. The interaction of RAMON with adjacent layers is based on *RAMON Primitives*. In the downward direction these primitives are interpreted by the pertinent A-plane; in the other direction, RPs act without any mediation since they are assumed compliant with the TCP/IP protocol suite. RPs are messages used by RAMON to interact with NC-planes and NU-planes. In this hierarchical model, the overall control of the radio access is assigned to the RAMON module. In Table 1, the key CPs are briefly described for the main layers interacting with RAMON.

5. Description of the RAMON algorithms

In this section we briefly describe some of the algorithms developed and implemented within the RAMON project. Their performance has been tested in a simulation platform fully compliant with the RAMON paradigm; this platform has been developed with *Network Simulator* (*ns*-2) and is described in Section 6. Results showing the performance of the proposed algorithms are shown in Section 7.

5.1. Mobility management algorithms

The RAMON module includes an abstract handover algorithm, running at the eMS, based on the virtualization of the functions necessary to support mobility. The abstract algorithm formulation has the purpose of making handover services programmable by the user and independent of the underlying technologies. The handover algorithm plays a central role in a scenario composed of wireless overlay networks, since the selection of the "best" access point at any moment is not simply related to the goodness of the current physical channel quality, but also implies a technology choice as a trade-off between performance, cost, power consumption, etc. Roaming across different systems also presents issues related to addressing and authentication, while keeping the

handover latency low to prevent adverse effects of TCP congestion control. All these features have been considered in the RAMON MM-c.

Similarly to [17,18], the handover control system requires two main functionalities:

1. handover decision,
2. handover execution.

The handover decision process includes trigger and detection functions. The trigger function has the role to individualize a condition in which it is necessary or convenient to start a handover, while the detection function has the role of choosing the best serving BS. The handover execution process is responsible for the detach from the old base station and for the attach to the new one. It includes control message exchanges and authentication/registration functionalities. From a functional point of view, handover decision and handover execution processes are completely decoupled. The handover control algorithm coordinates the calls of the abstract decision/execution primitives. By hiding the implementation details of the attach/detach functions and of the decision criteria from the handover control system, different decision mechanisms can transparently interface with different and multiple REs.

The handover execution process is based on interactions between RAMON module and Mobile IP agents. Our scenario is based on an all-IP architecture for the intrinsic capability of the IP protocol suite to decouple from underlying technologies.

5.1.1. Handover decision

The proposed control algorithm is based on a generic Mobile Controlled Handover (MCHO) style: Handover decisions and operations are all done at the eMS. The eMS keeps track of a list of Virtual Base Stations (VBS) in its coverage area. A VBS corresponds to an actual BS, [2] if the relative RE supports MCHO, or to a whole RE, for systems not supporting MCHO. In this case, the choice of a given VBS implies only a RE choice,

---

[2] Note that it is not an eBS.

and the final decision about target BS is taken by the RE native handover logic.

The handover decision criteria are based on performance parameters comparison. Periodically, for each VBS, the eMS collects CPs as QoS measures and makes these parameters comparable. VBS performance evaluation is based on (i) *user profile specifications*, which, according to user requirements, affect the decision metrics; (ii) *measurements*, which are used by detection algorithms on the basis of system-dependent available functions and signaling. The merit figure of a generic VBS_n at a given time is a function of the available bandwidth b_n, of the *distance d_n* between the VBS and the eMS, of the *power consumption p_n* in using VBS_n, of the *cost c_n* of the network to which the VBS_n belongs. While the last two parameters have fixed budgets and can be stored in an eMS archive for each RE, b_n and d_n have to be dynamically computed. We include available bandwidth information in the periodic advertisement message sent by BSs. For BSs not supporting the RAMON module, this information can be derived from "typical" values advertised by the BSs themselves. Indeed, eBSs estimate such a value on the basis of cell occupancy status and channel quality perceived by all admitted MSs [19]. Distance values are computed on the basis of the received signal power. The merit figure of the VBS_n is then evaluated as

$$f_n = w_b \cdot N(b_n) - w_d \cdot N(d_n) - w_p \cdot N(p_n) - w_c \cdot N(c_n), \qquad (1)$$

where w_b, w_d, w_p and w_c are the weights of each parameter, which sum to 1, and $N(x)$ is the normalized value of the parameter x. Note that, according to this formulation, in order to maximize the merit figure, distance, power consumption and cost have to be minimized. Weights can be modified by the user at run-time. As the eMS battery is dying out or the price approaches the spending limit, w_p or w_c, respectively, should increase dramatically to reflect such a condition. For those parameters that are not of concern to the user, weights can be set to zero. If high performance has to be pursued, we can assign $w_b = 1$, $w_d = 0$, $w_p = 0$ and $w_c = 0$: By maximizing the bandwidth, we achieve load balancing across different REs.
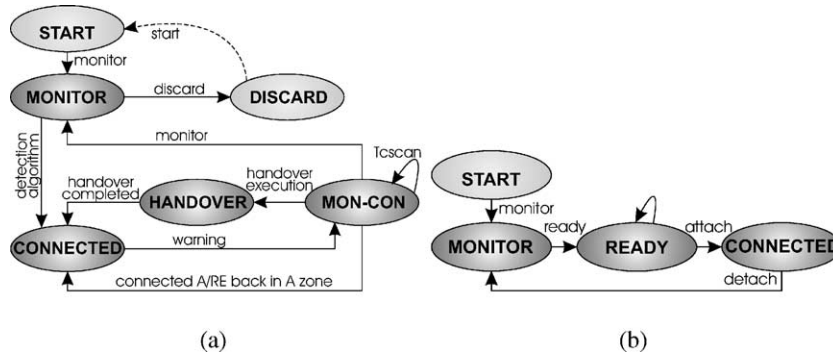
Fig. 3. (a) RAMON and (b) A/RE state machines for MM.

For each parameter b_n, d_n, p_n and c_n, to which we will refer as quality parameters in the following, an optimal and a critical threshold value have to be specified. These thresholds lead to three different operation zones: the best, the warning and the worse zone. If one parameter is not in the optimal range for a given period of time (*handover trigger timer*), a handover attempt is triggered. In such a condition, the merit figures of each available VBS are compared. VBSs with parameters worse than critical values, are not taken into account for the comparison. If a VBS results consistently better than the one in use during a given time interval (*handover detection timer*), the handover execution procedures are activated. An hysteresis value is added to the current VBS merit figure, in order to avoid handover operations for negligible QoS improvements. The RAMON API enables us to configure all the cited algorithm parameters: metric weights, timers, thresholds, and hysteresis.

5.1.2. Handover execution

Basically, logical mobility is supported by means of the *Mobile IP* protocol (MIP). The MM-c algorithm running at the RAMON module exploits MIP messages (*solicitations, advertisements, registration requests, registration replies*) in order to execute handover from one VBS to another. As we describe in the following, such messages are the result of MIP agent actions driven by RAMON logic. The MM-c algorithm may also inter-work with micromobility strategies, such as Cellular IP,

devised to hide local handovers from Home Agent/ Correspondent Nodes, thus reducing handover latency [20–27].

The MM-c algorithm involves the CC-plane, A-plane and NC-plane: The handover logic runs at the common control plane; native functionality extensions for such systems that do not support mobility (such as Bluetooth) are provided at the A/RE-*i* module; system-dependent functions and parameters are invoked at the NC-plane.

In the following we consider wireless systems not supporting MCHO paradigms; the general case can be obtained by substituting the RE with the VBS concept, as described in the previous section. Besides, for the sake of simplicity and without loss of generality, we consider the case of only two REs. From the MM point of view, the whole RAMON module and a generic A/RE can be represented as finite state machines, whose state diagrams are depicted in Fig. 3(a) and (b), respectively. In order to understand RAMON handover execution process we shall analyze actions performed by MM-c and A/REs. When the mobile node powers on, RAMON is in START state; according to the user requirements, the CC-plane sends a QoS request to the A-plane exploiting the α interface. Each A/RE-*i* becomes active and goes into MONITOR state searching for BSs in range.

Once a BS is found, A/RE-*i* goes to the READY state and it is ready to exchange data. The RAMON state machine is still in MONITOR state and can read the QoS level provided by the

A/RE-i using methods belonging to the α interface. According to the handover decision process, RAMON chooses the best RE, if one exists, otherwise it enters the DISCARD state, from which it can exit only if the user restarts the system. When MM-c decides to attach to the RE-i, it sends a suitable command to the A/RE-i and, in order to speed up the MIP registration procedure, sends a *MIP solicitation* (MIP-SOL) through the RE-i access network. After receiving the attaching command, A/RE-i goes into CONNECTED state and passes data and signaling packets to the upper layers. Thanks to the presence of a double protocol stack under the RAMON module, the other A/RE continuously tries to remain in the READY state, that is with all quality parameters at least in the warning zone, changing its point of access to the network, if needed. RAMON can perform a handover only towards a A/RE which is in READY state. This means that, the connecting and adapting procedures on the RE, to which RAMON may attempt to connect, run in background, that is before RAMON performs handover execution. This way, such procedures do not impact the overall inter-RE handover delay. When the A/RE is in CONNECTED state it continuously checks the CPs of the communication channel it is attached to. If one of the quality parameters goes under the optimal threshold, it notifies this event to MM-c, using a warning method. Once MM-c receives this warning, it sets the RAMON state into monitor-connected (MON-CON) and starts looking for a better RE, periodically reading (every *Tcscan* seconds) the quality achieved by the not connected A/RE. RAMON remains in MON-CON until (i) all quality parameters belonging to the connected A/RE are within the best zone again, (ii) both A/REs have a quality parameter at least under the critical threshold, (iii) MM-c decides to perform a handover. In the first case RAMON returns into CONNECTED state without changing RE. In the second case the MM-c module restarts the monitor phase. Finally, if the handover is triggered, MM-c sets the RAMON state to HANDOVER, notifies this event to TCP thus triggering the freezing procedure described in Section 5.2, and sends a MIP-SOL through the RE to which it is attempting to connect. The MM-c starts MIP registration and keeps on transmitting and receiving user data on the connected A/RE. Once a *MIP Registration Reply* (MIP-REG-REPLY) has been received back, MM-c calls attaching and detaching procedures to switch the communication between the REs; finally it notifies the end of the handover event to the TCP agent.

During data transmission, the RAMON module implements a packet filter as depicted in Figs. 4–6. In START, DISCARD and MONITOR state, RAMON discards all packets coming from either upper or lower layers, while, in CONNECTED and MON-CON state, packets flow only to and from the connected A/RE. When RAMON is in the HANDOVER state, instead, MIP signaling can also pass through the not connected A/RE, while user data continue to flow through the connected one. This allows the RAMON module to continue communicating during the handover procedure, till the MIP registration is completed. From this point of view the RAMON module does not have a significant impact on MIP handover delay, which may be
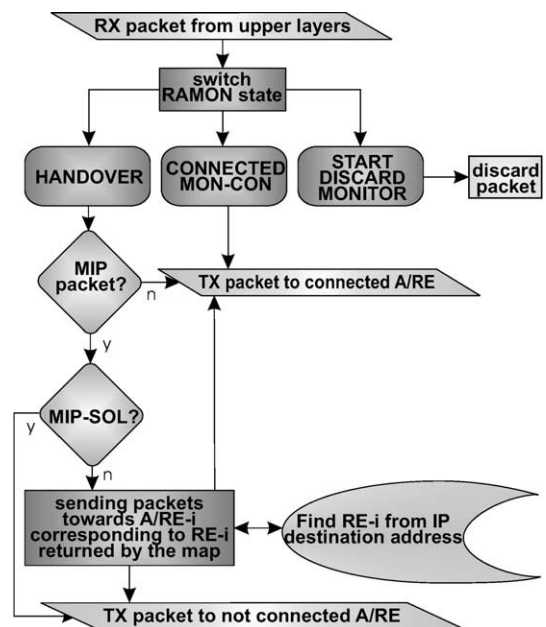

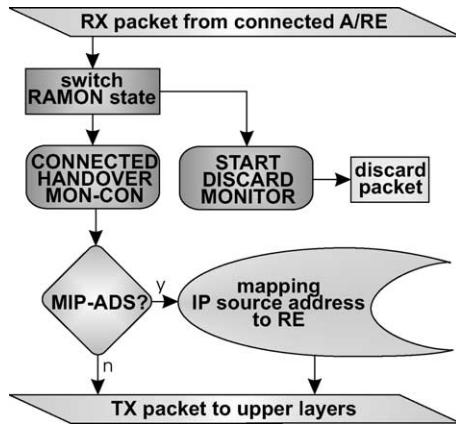Fig. 4. MIP packet filtering for packets coming from upper layers.

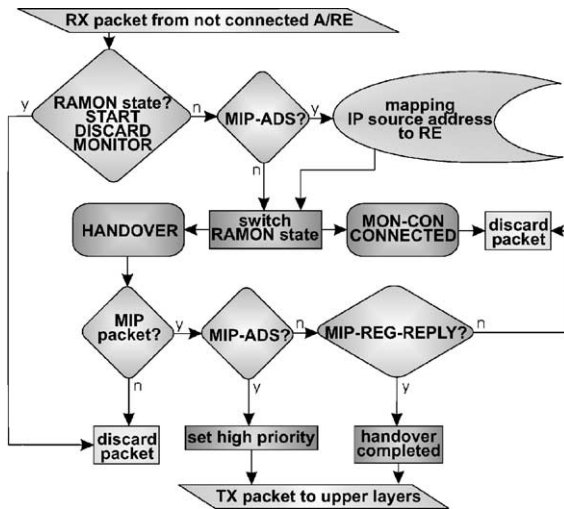Fig. 5. MIP packet filtering for packets coming from the connected A/RE.

Fig. 6. MIP packet filtering for packets coming from the not connected A/RE.

affected by the presence of *Tcscan* sampling timer, only when RAMON is in MON-CON state. This will be clearer in Section 5. Since the MIP agent is not aware of the presence of two different REs, and the RAMON filter does not stop *MIP advertisements* (MIP-ADV) originated by the not connected RE, MIP Foreign Agent selection could not match the MM-c RE choice. In order to prevent this undesired effect, MM-c maps the IP source address of the BS that has sent the MIP-ADV into the RE from which the MIP-ADV comes. Besides, when in HANDOVER state, RAMON internally marks

the MIP-ADV coming from the not yet connected RE with a high priority to force the MIP agent to register with the BS that sent the advertisement.

5.2. Session control algorithm

To guarantee *QoS session continuity* during handovers to an eMS migrating from an RE to another (inter-RE handover), a suitable Session Control algorithm has been designed at the SC-c. This algorithm is studied to enhance performance of the TCP protocol when disconnections occur frequently (in the following we name this protocol RAMON TCP New Reno). In this case, at least two problems may arise: The first one could be related to MIP registration delays, while the second is due to the intrinsically different link characteristics regarding the old and the new network. In the former case, during handover procedures, the eMS may be unreachable for time periods of the order of seconds. As a consequence, TCP timeout events may occur and performance is degraded. For what concerns the latter case, consider the situation where the round trip time of the new RE is much longer than the round trip time experienced by TCP in the old network. In this case, when the eMS is connected to the new link, TCP could erroneously time out due to the erroneous setting of the timeout timer. In fact, the timeout value is derived from old link measurements that are no longer valid when the eMS switches to the new RE. Note that, in both the cases, timeout events are due to incorrect timeout timer estimations rather than to congested or unaccessible links. After each timeout event, TCP forces the *Slow Start Threshold* (*ssthresh*) to *max* (*cwnd*/2, 2 *MSS*), where *cwnd* denotes the *Congestion Window* before timeout and *MSS* is the maximum segment size. Therefore, as the inter-RE handover is successfully completed, if a timeout occurs the sender enters the *Congestion Avoidance* phase and *cwnd* increases slowly causing a degraded throughput performance.

To cope with these problems, the TCP sender algorithm has been modified, still maintaining compatibility with standard TCP implementations. As stated above, after an inter-RE handover, path characteristics may change dramatically.

Consequently, what the TCP sender learned in terms of available bandwidth and round trip time is no longer valid [28]. Based on this observation, after the inter-RE handover is completed, the RAMON entity resets TCP sender CPs (i.e., SSHTRESH, SRTT, and RTO), and enters into the so-called *Fast Learning* phase during which it rapidly estimates the available bandwidth and the round trip time for the new link. Moreover, to avoid useless segment transmissions, the SC-c algorithm monitors the TCP status during handovers; TCP is stopped when consecutive timeouts are observed. The normal transmission mode is then restored at the end of the handover procedure. The information about the beginning and the end of handovers is provided by lower layer notifications through RPs. RE handovers. We stress the fact that our scheme is effective when the TCP sender entity is at the eMS. In fact, it is the mobile that has the perfect knowledge of ongoing handover status and that can *freeze* and *restore* correctly the TCP layer through the RAMON entity. When the TCP sender is not the eMS, a similar behavior can be obtained as explained in the following. Before initiating the handover, the eMS generates an ACK containing a *Receiver Window* (*rwnd*) field equal to 0. This results in a *freezing* of the TCP sender and avoids consecutive timeouts expirations. When the handover is completed, the TCP receiver at the eMS generates a new ACK with the original value of *rwnd*: this occurrence resumes the communication. Note that this algorithm can solve the problem due to the latency of MIP or to any other additional delay needed to set up the new link, but it is ineffective against round trip time differences among networks. The only way to solve this problem would be to modify the TCP algorithm at the sender as well.

5.3. Radio resource control algorithms

As previously indicated, the RAMON algorithm may also involve radio resource control operations. In particular reconfigurability can be used to achieve desired QoS requirements in terms of information integrity and energy consumption and also to obtain an efficient use of RE radio resources. While the former goal can be obtained by exploiting reconfigurability in the error control algorithms implemented at an eMS (Section 5.3.1), an efficient use of radio resources through reconfigurable approaches is accomplished by involving both eMSs and an eBS (see Section 5.3.2).

5.3.1. Error control algorithm

To preserve information integrity of packet transmission over the radio channel while meeting the desired QoS and energy constraints, an algorithm has been developed within the RAMON RRC functional set. The algorithm provides optimal operational conditions and parameter setting at the RLC layer. Consider an uplink traffic connection between an eMS and a BS. We assume that a generic RLC/ARQ protocol is implemented (e.g., the acknowledged transfer mode described for the UMTS RLC protocols) and error control is performed by means of positive and negative acknowledgments. The proposed algorithm consists of two parts.

The objective of the first part of the algorithm is to determine the value of the *maximum number of retransmissions per PDU* (MAX_LINK_RETR) at the RLC layer, such that a target value P_t of the packet loss probability at the transport layer is guaranteed [29]. Since we would like to dynamically adapt MAX_LINK_RETR to the channel conditions, we derive a simplified expression which provides MAX_LINK_RETR as a function of P_t, the mean transport layer packet size (TRANS_PACKET_SIZE) and the error process at the link layer (i.e., BURST_ERR and ERR_PR). Losses of different RLC PDUs are assumed to be independent and to occur with the same probability. The value of MAX_LINK_RETR is passed as a CP from the CC-plane to the NU-plane (downward sharing).

The second part of the algorithm aims at trading-off energy consumption with traffic delay, by controlling the operational state of the transmitter at the eMS. The sender detects that the radio channel conditions are bad upon receiving a retransmission request. In this case, the RAMON entity can choose between two ARQ schemes: *greedy* or *saving* mode. In the *greedy* mode, the sender retransmits the missing PDUs immediately and then goes on with the information transfer. In the *saving* mode, upon the retransmission request

arrival, the sender stops transmitting after the current transmission has been completed. The sender starts polling periodically the receiver to probe the channel status, and resumes the data transfer when it receives a reply. The saving mode is introduced to let the system "save" radio resources, as well as energy, in the case of bad channel conditions. At the cost of a higher energy consumption, greedy mode is more reactive than saving mode to changes in the channel conditions, and therefore is able to provide better QoS. In order to dynamically trade-off between the needs of QoS and energy saving, a control mechanism on the sender is introduced: if the number of PDUs in the RLC buffer (QUEUE_LENGTH) is less than a given threshold T_h, the RAMON entity sets the sender to operate in saving mode, otherwise it enters the greedy mode. Under low load conditions, which are not critical for QoS provisioning, energy saving is privileged; on the contrary, when the queue fills up and QoS deteriorates, QoS provisioning is favored. By varying the value of T_h, the desired trade-off can be established between energy saving and traffic QoS as the channel conditions and the energy status of the eMS change.

5.3.2. Resource sharing algorithm

We defined a generic radio resource allocation scheme that could be easily adapted to REs with different radio interfaces and different radio allocation procedures. [3] The key purpose is to have at the RAMON module the flexibility of designing scheduling disciplines that can be employed in different REs thanks to reconfigurability and the mediation of the adaptation layers. This reconfigurable framework, named CHannel Adaptive Open Scheduling (CHAOS), defined in [30], is part of the RRC-c and mainly resides at the eBS. CHAOS provides a framework for the design of scheduling strategies for efficient resource sharing and adaptation to (i) *traffic* conditions; (ii) *physical channel* conditions. Different CPs may be chosen to represent both variables: Traffic conditions may be represented by transmission buffer occupancy

(QUEUE_LENGTH) or queue age associated to packets in the transmission buffers (QUEUE_AGE); channel conditions may be expressed by SIR and/or average *Packet/Frame Error Ratio* (ERR_PR). CHAOS divides capacity requests into classes based, for example, on SIR values and queue age of packets in transmission buffers. The requests are then expressed in a *matrix*, where the columns represent different classes of channel quality and the rows indicate different classes of traffic level. Different priorities, related to traffic or channel quality, can be defined to scan the matrix. Thus, different scheduling algorithms can be identified on a CHAOS matrix depending on weights given to the two components, which result in different serving patterns on the matrix, i.e., in different allocation strategies. The output of the overall process is capacity assignment to the different MSs (either standard MSs and eMSs).

Fig. 7 shows the basic information flow, i.e., how the CHAOS entity running at the eBS CC-plane gathers information about system state (for sake of simplicity we consider a single cell composed of M mobile stations). For every MS, in both directions, the RRC-*i* (relative to the *i*th RE) entity in the NC-plane of the eBS collects information that will be used for the evaluation of the abstract parameters by the A-plane. The RRC-*i* entity on the eBS gets the BS-related information directly from the different layers of the NU-plane (i.e., the RLC-*i*, MAC-*i* and PHY-*i* layers). Information lying in the MS has to be exchanged between the two RRC peer entities (MS RRC-*i* and eBS RRC-*i*) by means of the transport facilities offered by lower layers. As soon as new information describing the system state is acquired by the eBS RRC-*i*, a *CP UPDATE indication primitive* (1), which is RE-dependent, is issued to the A-plane. Mapping of these RE-dependent parameters into abstract parameters (CHANNEL STATE and TRAFFIC CONDITION), that can be used by the CHAOS algorithm, is up to the A-plane, which asynchronously communicates the abstract parameters to the CC-plane entity as soon as they are available, by means of an RE-independent *CP UPDATE primitive* (2). The A/RE-*i* entity asynchronously issues RE-independent *CAPACITY ASSIGNMENT REQUEST*

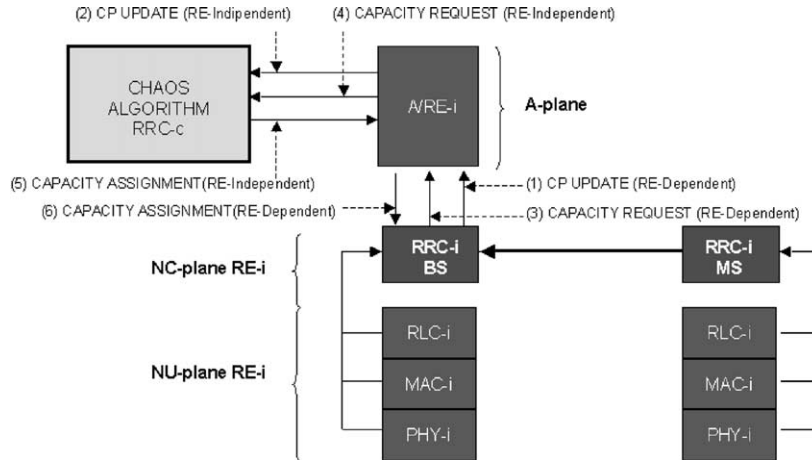[3] The algorithm requires the RAMON entity to be at the BS, i.e., an eBS.

Fig. 7. Description of information flow from U-plane to CC-plane.

primitives (4) to the CHAOS entity in the CC-plane. These abstract requests are formulated by the A/RE-*i* plane on the basis of the RE-dependent explicit request coming from the RRC-*i* (RE-dependent *CAPACITY REQUEST primitive* (3)) or on the basis of the CPs gathered when no explicit requests are issued by native system control mechanisms. These primitives contain the overall amount of capacity to be assigned. The CHAOS entity processes this request and returns an ordered vector of length M whose element contains the MS identifier and the amount of capacity assigned to it through the RE-independent *CAPACITY ASSIGNMENT primitive* (5). The last step (6) consists in the A/RE-*i* entity translating the assignment into an RE-dependent *CAPACITY ASSIGNMENT primitive* command that can be issued to the eBS NC-plane. This will

result in the actual assignment with NC-plane specific mechanisms.

We conclude this section by describing how the CHAOS entity uses system state information to assign capacity to the different MSs. As soon as *CAPACITY REQUEST primitives* arrive from the A/RE-*i* plane, this information is arranged in a matrix. In Fig. 8 the CHAOS matrix is shown with three different scanning methods. The horizontal dimension represents the channel state, and thus requests with a different value of CHANNEL STATE occupy different positions in the matrix. The vertical dimension is associated with traffic condition, thus requests with different values of TRAFFIC CONDITION are put in different vertical positions in the matrix. What the CHAOS entity obtains is thus a two-dimensionally ordered description of the requests coming from different
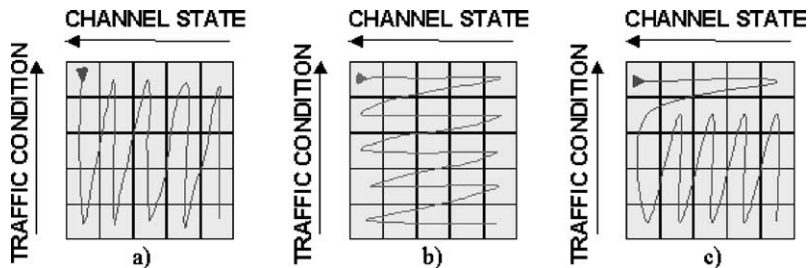

Fig. 8. The CHAOS matrix. Examples of matrix scanning methods.

MSs. User requests are served in the order defined by a predefined rule (scanning method). Each different rule results in a different scheduling discipline. In Fig. 8(a) the matrix is scanned by column by giving priority to traffic state conditions; in Fig. 8(b) it is scanned by row by giving priority to channel state conditions; a combination of the first two methods is shown in Fig. 8(c).

6. The simulative approach

In this section the structure of the *ns*-2 RAMON simulator (Fig. 9) is presented with reference to UMTS-TDD, 802.11 and Bluetooth REs. The simulator is based on the `ns` package [31] (ver. 2.1b7a). Specifically, modifications have been carried out to the Wireless Node object (*MobileNode* class). One protocol stack for every simulated RE is implemented in the same MobileNode object.

The RAMON module and the A-plane modules are interposed between Agents (RTAgent, MIP Agent, etc.) and radio access layers (LL, MAC,

etc.). On the left part of Fig. 9 the UMTS-TDD protocol stack is shown with its specific Adaptation plane (A/RE-UMTS in figure). The 802.11 and the Bluetooth stacks are on the right side with their A-planes (A/RE-802.11 and A/RE-BT). On top of the stacks the RAMON module is directly linked to the TCP (or UDP) layer, to the *Mobile IP* (MIP) layer and to the NOn AdHoc routing agent (*NOAH* routing agent) [32].

While the 802.11 protocol stack is natively implemented in the *ns*-2 simulator, the UMTS-TDD protocol stack has been fully developed in the RAMON project. The BT protocol stack is derived from the `ns` *Bluehoc* simulator [33] and modified to adapt the Bluetooth node object *BTnode* to the `ns` MobileNode object. The α interface in Fig. 9 defines the messages exchanged between CC-plane and A-planes. The functions of the α interface can be related to RPs and the parameters they exploit to the CPs. Specific functions have been associated to each message exchanged through this interface. A list of the most important functions is given in the following:
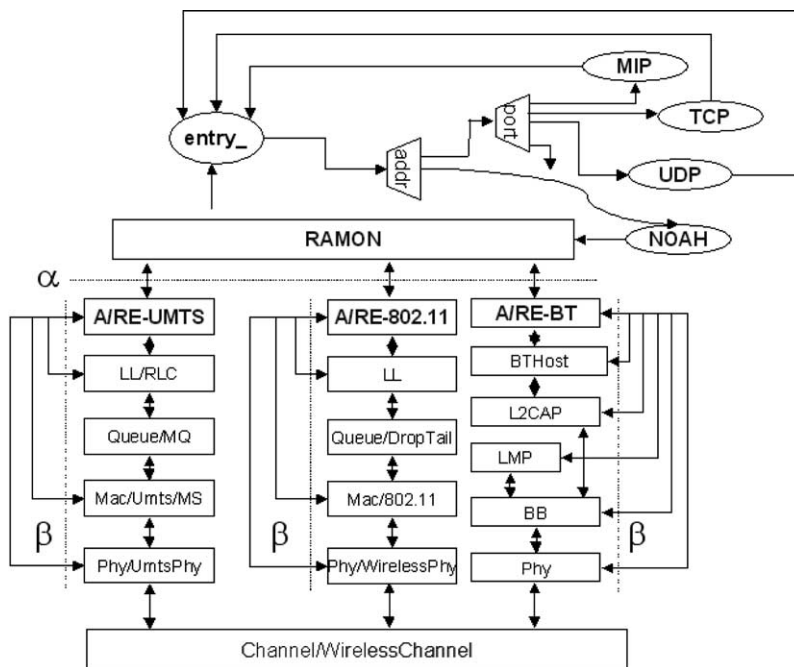

Fig. 9. Overall simulator architecture.

- `get(parameters_name)` gets the `parameters_name` value from lower layers.
- `attach` is used to connect the MS to a new network. In more detail, it provides an *IP context* for the MS and registers the node to the Mobile IP *Foreign Agent* (*FA*).
- `detach` disconnects the MS from a network and cancel the registration from the FA.
- `monitor(RE)` returns a quality metric for a specific RE. This metric is used to drive handover procedures.
- `set(parameters_name,value)` sets the `value` value to `parameters_name`. It is used by the RAMON module to set lower layers' parameters.
- `send(packet,options)` sends regular and control packets to lower layers. Control packets are used by RAMON algorithms to dynamically adapt lower layers behavior to network dynamics and user requirements.
- `receive(options)` receives data packets.

In particular, the "`get`" function is used by RAMON algorithms to read CPs from the A-planes for optimization purposes. As described in Section 4, CPs originated at different layers can be associated to different optimization tasks, for example (i) physical layer CPs are related to power control and energy saving; (ii) link layer CPs are associated to link reliability and packet delay; (iii) transport layer CPs are related to the QoS perceived from the user application in terms of packet delay and throughput. The "`set`" function is needed to pass some values to the A/RE-*i* modules: With this primitive, some CPs can be modified by the CC-plane. Both the "`set`" and the "`get`" functions are also defined for the interaction with the transport layer protocols (e.g., TCP and UDP). Two more primitives are defined for interaction between CC-plane and the transport layer:

- `start_handover_notification`
- `end_handover_notification`

They are used to notify the RAMON SC-c about the beginning and the end of a handover event (see Section 5.2).

7. Performance issues

In this section we report some performance results measured in the RAMON simulation. It is worth noting that the main result is the demonstration that the RAMON module can perform reconfiguration across heterogeneous wireless technologies without losing IP session continuity. First, we show MM-c and SC-c performance in two different situations:

1. forced inter-RE handover,
2. user-driven handover.

These scenarios are relevant in the RAMON context because they easily demonstrate how a CC-plane can react to variations perceived by means of CPs, in the REs that the CC-plane handles. Then, we show the RRC-c performance.

7.1. Forced inter-RE handover

Let us assume that an eMS is within the coverage area of two different REs: UMTS and Bluetooth; it loses connectivity and is forced to attach to another RE in order to maintain session continuity. Since we aim at measuring performance of a forced handover, we set the handover decision weight at $w_b = w_c = w_p = 0$ and $w_d = 1$. Fig. 10 depicts the considered topology. An eMS moves to and from one UMTS BS and one Bluetooth Access Point (AP) in a ping-pong fashion, remaining for about 10 s near each BS before moving towards the other one. The distance between the two BSs is 58 m. The simulation time lasts 10,500 s. The eMS is loaded with a FTP source over a TCP New Reno or a RAMON TCP New Reno transport protocol (see Section 5.2) and communicates with a correspondent host through an IP router, common to both the RE access networks. We assumed that the UMTS BS acts as MIP *Home Agent* (HA) and the BT AP as *Foreign Agent* (FA). Delay values for the wired links that connect BSs to the common router, are chosen so that the eMS perceives a round trip time of 0.3 and 1 s in the UMTS and BT access networks, respectively. As for Bluetooth, we chose a radio device of class 2 [34], while the inquiry scan offset
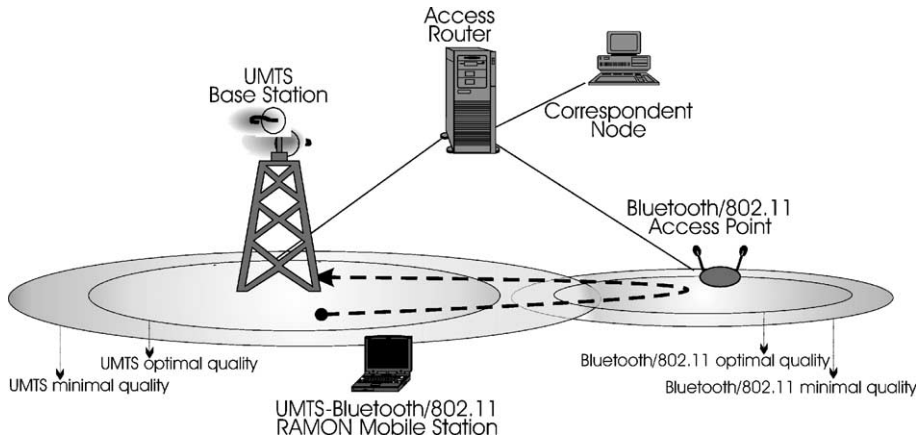
Fig. 10. Topology used in simulations.

timer for the AP has been set to 2 s. As regards UMTS, we chose TDD operational mode with six slots dedicated to uplink, thus resulting in a maximum uplink throughput of 768 kbit/s. A dedicated function in the A/RE translates the RE dependent physical quality parameters into an equivalent virtual distance from the BS, called d_n in Section 5.1.1. As for UMTS, d_n optimal and critical thresholds correspond to a received SIR of 6 and 2 dB, respectively, while, as for BT the correspondence is with values assumed by *Re-ceived Signal Strength Indicator* (RSSI) [34] when the eMS is 6 and 8 m distant from the AP. Simulation results are shown in Fig. 11(a) and (b). We report average inter-RE handover delays vs. MON-CON timer (*Tcscan*) and average throughput vs. TCP timeout estimator granularity (*TCPTick*). For the average handover delays we provide confidence intervals calculated with 70 samples and a confidence level of 95%, while average throughput values refer to 10,500 s simulation time. Simulations show that there is a
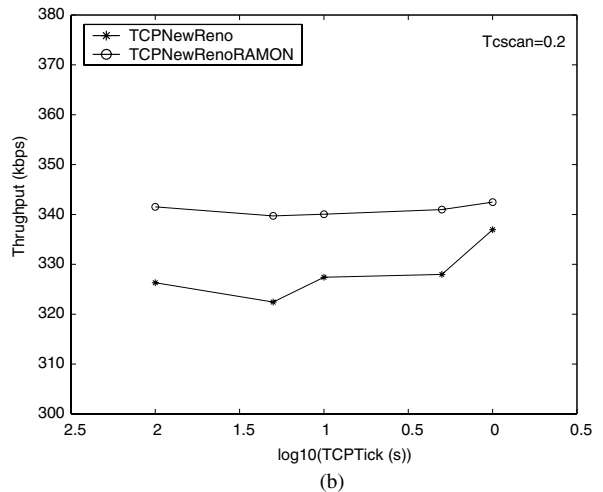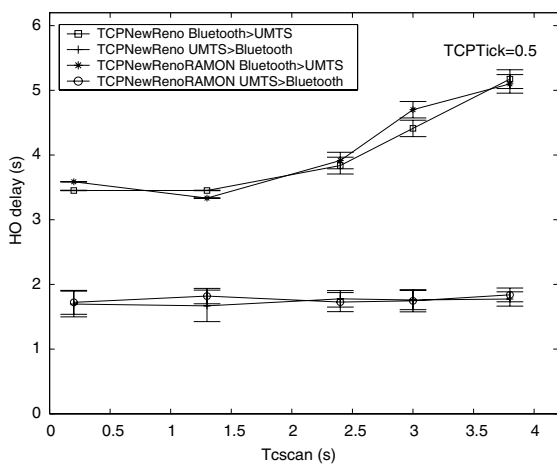

Fig. 11. (a) Average inter-RE handover delay vs. MON-CON timer and (b) user average throughput vs. TCP timeout estimator granularity.

certain gain in terms of throughput, passing from classical TCP New Reno to RAMON TCP New Reno. The reason is related to the freezing mechanism described in Section 5.2. Moreover, passing from BT to UMTS, performance degradation occurs as $Tcscan$ increases. In fact, since UMTS radio coverage degradation is smoother than Bluetooth, as distance from a BS increases, during an inter-RE handover from UMTS to Bluetooth, the eMS can maintain connectivity within UMTS until Bluetooth is able to transmit user data. On the other hand, when eMS moves from BT to UMTS, as RAMON becomes MON-CON with RE-Bluetooth, the radio coverage is suddenly lost before the $Tcscan$ timer expires, resulting in a greater handover delay, increasing as $Tcscan$ becomes larger.

7.2. User-driven handover

Here we chose UMTS and 802.11 as REs; several eMSs are in the coverage area of both REs at the same time and choose the best BS, evaluating a cost function as described in Section 5.1.1. Our purpose is to demonstrate how user profile specifications affect handover trigger and detection phases. In fact, the optimization of different performance figures requires different choices in terms of RE attachment/detachment policy. For example, if the user's main goal is cost saving, connections to low-price access points have to be maintained as long as possible, even if better transmission conditions (in terms of bandwidth or channel quality) towards other stations are available.

In our simulations we consider an area in which heterogeneous radio access technologies (namely UMTS and 802.11), experiencing different traffic conditions, overlap. In particular, we have considered a simple network topology: four 802.11 BSs (referred to as BS_2, BS_3, BS_4, BS_5) are placed at the vertices of a square and a UMTS BS (BS_1) is placed in the center. The side of the square is set to 250 m, while the coverage area of the 802.11 and UMTS BSs are set to 100 and 1000 m, respectively. Channel rate in 802.11 cells is set to 2 Mb/s. 802.11 BSs have a different number of attached users: Four eMSs are connected to BS_2 and BS_4, while one eMS is connected to BS_3 and BS_5.

In a simulation run, an eMS, involved in a 15 Mbytes file transfer from the fixed network, moves clock-wise at 2.5 m/s along the square starting from a vertex, for example from BS_2. Although during the simulation time the eMS is covered by BS_1, handover to 802.11 BSs can be performed in order to save power or to reduce cost. According to the considered load scenario, 802.11 BS_2 and BS_4 offer an amount of available bandwidth lower than UMTS BS_1, while BS_3 and BS_5 offer a higher amount of bandwidth. The required user trade-off is expressed by the decision metric (Section 5.1.1) settings. We compute such a metric considering distance, price and bandwidth offered by each BS.

In order to make heterogeneous system parameters comparable, a normalization function is required: Distance is expressed as the ratio between actual distance and nominal RE-dependent coverage radius d_{nx}, price and bandwidth are normalized with respect to the maximum inter-RE values c_x and b_x. In particular, we assume that the cost to transfer 1 Mbyte of data is 1 for UMTS, 0.5 for 802.11, while b_x is set to 1 Mbit/s. The final metric is given by a linear combination (*linear metric*) of such normalized parameters with coefficient w_i:

$$f_n = w_b \cdot \frac{b_n}{b_x} - w_d \cdot \frac{d_n}{d_{nx}} - w_c \cdot \frac{c_n}{c_x}. \qquad (2)$$

Optimal and critical thresholds are summarized in Table 2.

We recall that handover is triggered when one of these parameters is in the warning region, and that BSs with parameters worse than warning values are not considered in the decision phase. In our simulations, we set the metric distance weight to 0.3 and we observe performance results varying the cost and bandwidth weights according to the relation $w_b = 0.7 - w_c$. Each setting corresponds to a different handover policy (in terms of hand-

Table 2
Threshold values adopted in the simulation

Parameter	Optimal region	Warning region
b_n	$b_n > 0.2 \cdot b_x$	$0.05 \cdot b_x < b_n < 0.2 \cdot b_x$
d_n	$d_n < 0.8 \cdot d_{nx}$	$0.8 \cdot d_{nx} < d_n < d_{nx}$
c_n	$c_n < 0.8 \cdot c_x$	$0.8 \cdot c_x < c_n < c_x$

over trigger instants and attachment choices) and consequently to a different QoS performance. QoS performance is expressed by the time spent for the file download and by the total amount of the cost.

We analyze preliminarily single simulation experiments in the extreme situations in which we want to minimize the transfer time regardless of the cost ($w_c = 0$) or, conversely, we want to minimize the file transfer cost regardless of the transfer time ($w_c = 0.7$). The top graph and the bottom graph of Fig. 12(a) show the handover trigger and decision policies resulting in the extreme cases considered. We report the identifier of the selected BS vs. the simulation time. In the $w_c = 0.7$ situation, the connection to WLAN is kept as long as possible, since this access technology is the cheapest (handovers are triggered only when the eMS moves outside the coverage area of an 802.11 BS). Indeed, in the $w_c = 0$ case, the RAMON node remains connected to the BS that offers more bandwidth as long as possible (switch to WLAN BS_2 and BS_4 does not occur since such stations are very loaded). The figure also shows an intermediate case in which w_c is set to 0.3. In this case, handovers to BS_2 and BS_4 are performed, but the connection time in such cells is lower than in BS_3 and BS_5, since our metric accounts for both distance and load. Fig. 12(b) visualizes the effect of each decision criterion on the file transfer rate. Filtered bandwidth samples are plotted vs. the simulation time. Samples are evaluated every 0.1 s, and a simple AR filter with a memory α coefficient

equal to 0.9 is adopted. From the figure we note the UMTS always offers a very reliable service, while WLAN bandwidth fluctuations are relevant.

In order to quantify the performance of a given decision metric in the considered network scenario, we ran 30 different simulations for each weight setting. The average time and cost resulting for a 15 Mbytes file transfer is reported in Fig. 13(a) vs. the w_c value. Error bars refer to a confidence interval of 95%. This figure shows that, by changing the weights of the cost function, the RAMON user can effectively configure its optimal cost/performance trade-off. Even if the minimum/maximum percentage deviations of the time curve and of the cost curve are different, a symmetrical behavior is evident.

Finally, we investigated the effects of alternative definitions of the decision function. According to previous metric formulation, the metric comparison is based on the weighted difference between the parameters of interest. It could be more appropriate to base such a comparison on their ratio. For example, supposing $w_c = w_b$, if a network offers twice as much bandwidth, but twice as expensive as another network, the user could consider these networks as equally good. The property of logarithm $\log a - \log b = \log(a/b)$ can reflect this logic. We define a second metric (*logarithmic metric*) as follows:

$$f_n = w_b \cdot \log \frac{b_n}{b_x} - w_d \cdot \log \frac{d_n}{d_{nx}} - w_c \cdot \log \frac{c_n}{c_x}. \quad (3)$$
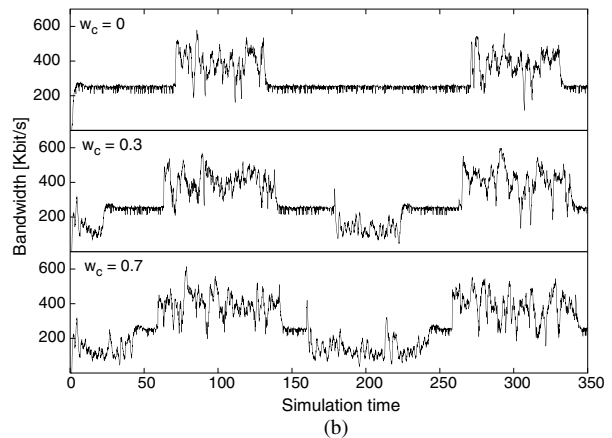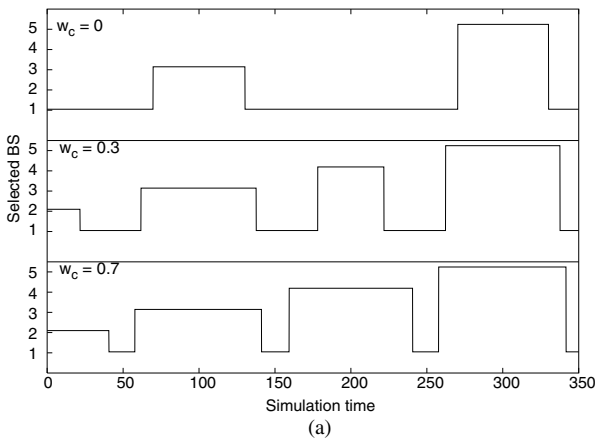

Fig. 12. (a) Different handover policies and (b) relative obtained bandwidth vs. simulation time in the case of linear metric.
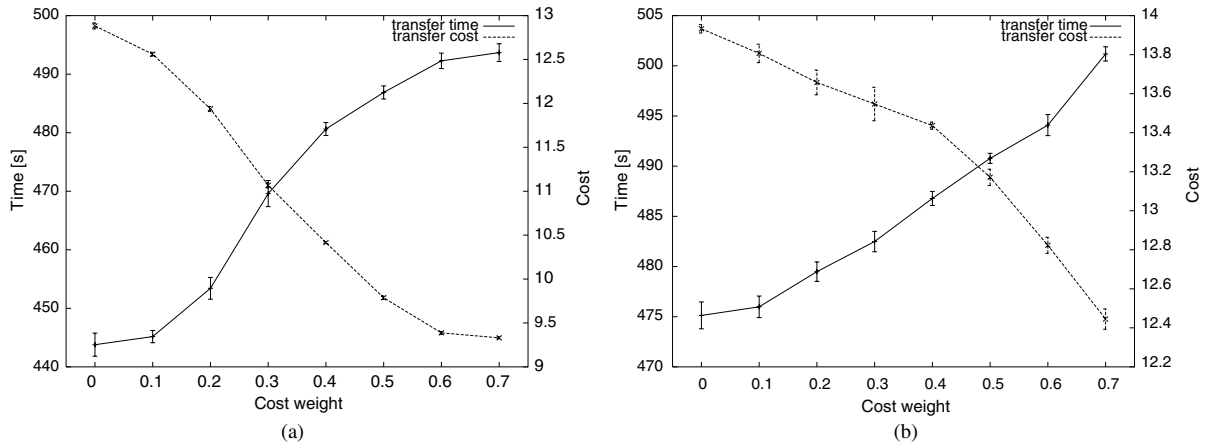
Fig. 13. Transfer time/transfer cost trade-off varying w_c parameter in the case of (a) linear metric definition and (b) logarithmic metric definition.

Fig. 13(b) shows the time/cost trade-off obtained with the logarithmic metric, in the same network and simulation conditions described for Fig. 13(a). The behavior of the curves in 13(b) is similar to 13(a), but the performance is worse for each weight setting and maximum/minimum ranges are reduced.

This phenomenon is due to the fact that, in the considered scenario, UMTS coverage is always very good and WLAN performance better only when the user is very close to the WLAN BSs (even if w_c or w_b is high). Thus, as we can see in Fig. 14(a) and (b), the overall performance is less sensitive to w_c and w_b settings. Although a logarithmic metric gives worse performance in our demonstrative scenario, we argue that it can be effective in realistic situations, in which inter-RE handover should be performed only for significant QoS improvements.

7.3. Link layer parameter setting

In this section, we present some results showing the performance that can be obtained at the transport layer by properly setting the link layer parameters. We consider the UMTS RE and apply the first part of the algorithm described in Section 5.3.1. Recall that the goal is to determine the maximum number of retransmissions per Protocol

Data Unit (PDU) at the RLC layer (`MAX_LINK_RETR`), such that a target value, P_t, of the packet loss probability at the transport layer is guaranteed.

We assume that the peak data rate over the wireless link is equal to 384 kbit/s and the PDU size at the link layer (`LINK_PACKET_SIZE`) is equal to 480 bytes. The TCP maximum window size is equal to 20 transport layer packets, and the average *on* and *off* periods of the application are equal to 1 s. We assume that the average delay perceived by packets in traversing the wired network is equal to 100 ms, while we neglect losses due to the wired network. We focus on the system performance when the TCP data packet size is constant and equal to 1000 bytes; in this case, each TCP packet is divided into three PDUs at the link layer.

We operate as follows: Through the proposed algorithm we compute the maximum number of retransmissions at the RLC layer which guarantees the desired packet loss probability at the transport layer, given the error process at the link layer (i.e., `BURST_ERR` and `ERR_PR`). Then, we set the `MAX_LINK_RETR` parameter at the RLC layer to the obtained value and, by employing the RAMON simulator, we derive the mean packet delay at the transport layer. Fig. 15 shows the trade-off existing between P_t and the TCP packet
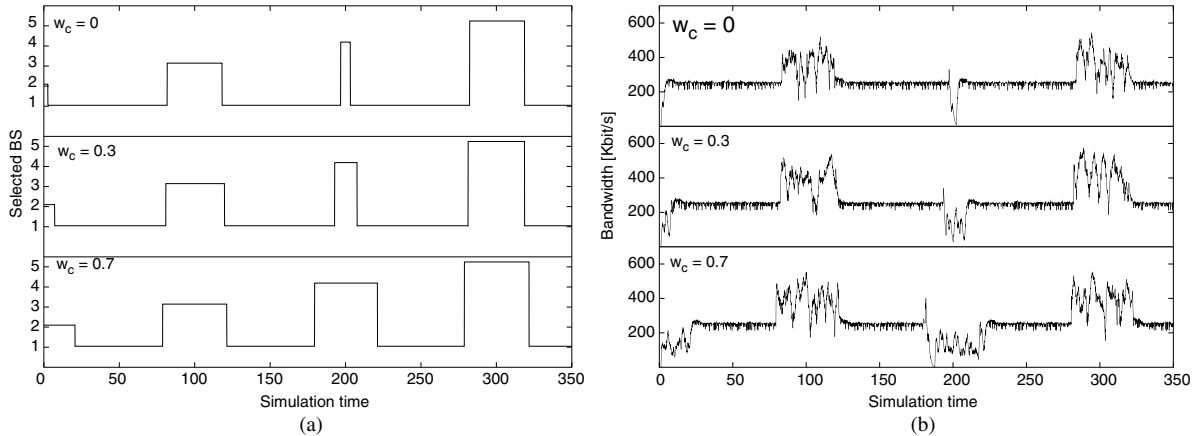
Fig. 14. (a) Different handover policies and (b) relative obtained bandwidth vs. simulation time in the case of logarithmic metric.

delay, for different values of the average PDU error probability. Given a certain value of error probability, smaller values of P_t can be obtained by increasing the maximum number of retransmissions at the RLC layer. This implies larger delay of the TCP packets; in particular, for increasing values of the error probability, the packet delay significantly grows as P_t decreases. As an example, for an average PDU error probability equal to 0.3, the mean delay at the transport layer increases of 50% when the target loss probability varies from 10^{-1} to 10^{-3}.

7.4. Radio resource sharing

In this section results concerning improvements that can be achieved with the CHAOS strategies are shown for the UMTS and for Bluetooth separately. As said before, it is important to notice that CHAOS constitutes a large class of algorithms and, by modifying the matrix scanning methods, different service disciplines (with different targets) can be easily achieved.

In the UMTS-TDD simulated scenario M mobiles in a single cell send data through a gateway to M wired nodes. The entire data traffic is in the uplink direction. In the UMTS frame nine timeslots have been statically allocated to the uplink (1 for the RACH and 8 for the USCHs), and the remaining six have been allocated to the downlink
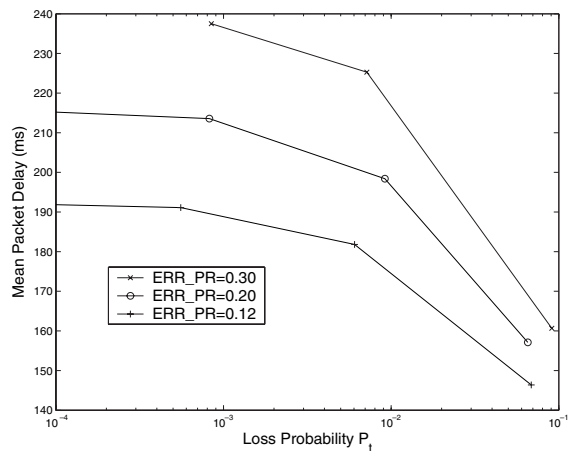

Fig. 15. Mean packet delay vs. target packet loss probability at the transport layer, for different values of the average PDU error probability.

(1 for the FACH and BCH and 5 for the DSCH); thus, the maximum attainable throughput in the uplink direction is 1024 kbit/s. The traffic is generated by FTP traffic sources (one FTP agent per node) at the TCP transport layer.

Three matrix scanning methods have been used in the simulations: the first one, named *Random*, scans the matrix randomly; the second one, named $CHAOS_1$, scans the matrix by giving priority to the oldest requests (see Fig. 8(b)), and the last one, $CHAOS_2$, gives priority to the requests from users
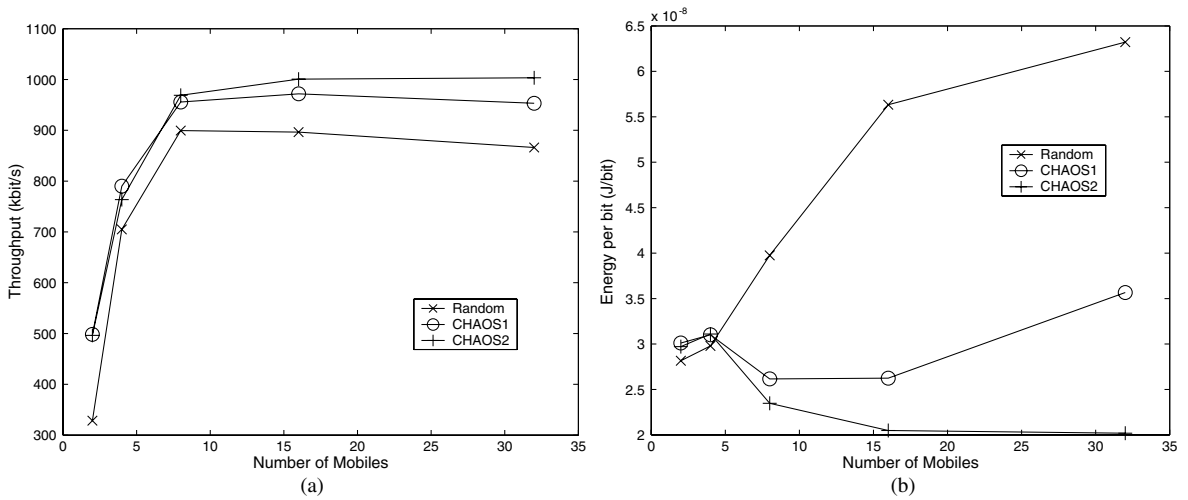
Fig. 16. (a) FTP throughput and (b) energy per bit vs. number of MSs varying matrix scanning methods.

with better channel quality (see Fig. 8(a)). In Fig. 16(a) we can see that throughput is maximized by giving priority to "best channel" requests. This throughput gain is due to more efficient use of the radio interface: The adoption of a channel adaptive scheduling decreases the RLC-PDU error probability, leading to a better exploitation of the radio resource. This in turn reduces the need for packet retransmissions: With the $CHAOS_2$ discipline the probability of successful transmission at

the first attempt is 0.998 vs. 0.957 for the *Random* case. Fig. 16(b) illustrates the gain in energy efficiency brought about by the use of a channel-adaptive packet scheduling algorithm. This result can be explained by observing that, with the CHAOS algorithm, mobiles tend to transmit more during the intervals in which they experience a high channel quality, when the transmitted power is reduced by the power control algorithm. Moreover, the decrease in the number of retrans-
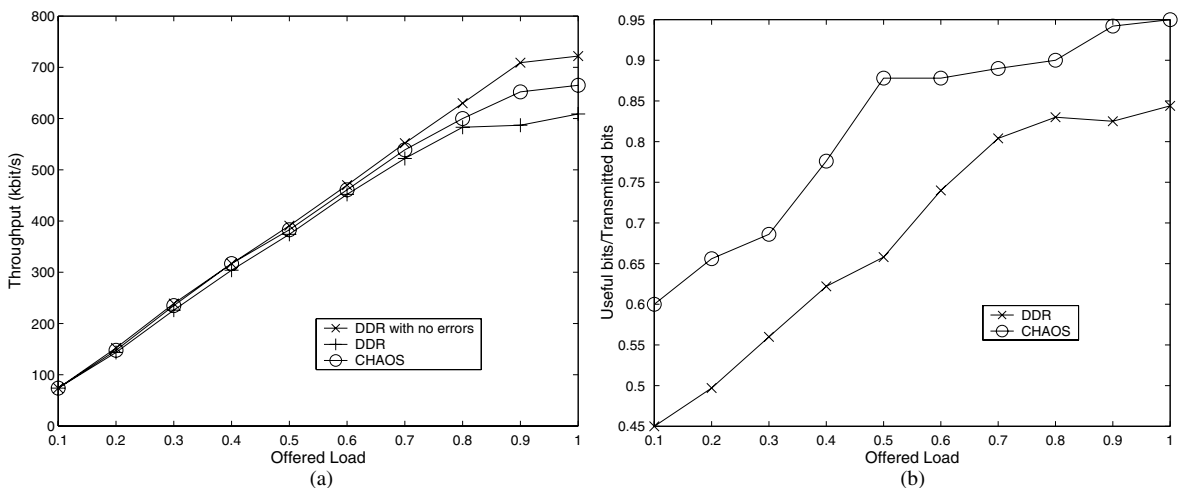

Fig. 17. (a) Throughput and (b) received bits/transmitted bits vs. offered load with different scheduling disciplines.

missions also contributes to the increase in efficiency.

The BT simulation scenario involves a piconet with one master and two slaves. Two different CBR connections are supported in the downlink direction (from master to slave), and transport and network layer protocols are, respectively, UDP and IP. The channel is modeled as a two-state Markov chain: In the BAD state the *Packet Error Rate* is very high (90%), whereas in the GOOD state no errors occur on the channel. Permanence time in each state is exponentially distributed with mean value equal to 5 s in the BAD state and 20 s in the GOOD state. This model accounts for interference from co-located 802.11b devices. Fig. 17(b) shows the number of information bits received with respect to information bits transmitted obtained by varying the offered load to the piconet. This value can be interpreted as a measure of power efficiency since for low power devices (class 2) no power control is used. It can be observed that while CHAOS constantly outperforms the Deficit Round Robin (DRR) scheduler, higher values of power efficiency are obtained when offered load increases. This mainly happens because when much free capacity is available (which happens for lower values of offered load) useless retransmissions occur, which fail because the channel is in the BAD state.

8. Conclusions

In this paper we introduced a reconfigurable module, named RAMON, able to operate in different mobile communication environments and to support computing applications based on the TCP/IP protocol suite. The paper mostly concentrates on architectural issues in the common control plane where RAMON is located. We described the RAMON control algorithms that constitute the processing core of the module and we indicated the interactions of these algorithms with different mobile systems like UMTS, Bluetooth and 802.11. To illustrate some of the advantages provided by the RAMON module we tested it by a simulator implementing, besides the

RAMON control functions and interfaces, the main functional settings of the aforementioned wireless systems. Several performance results are shown corroborating the proposed approach for reconfigurability.

References

[1] A. Roveri et al., The RAMON module: architecture framework and performance results, in: Proc. of QoS-IP 2003, Milan, February 2003, pp. 471–484.

[2] A. Baiocchi et al., Reconfigurable packet scheduling for radio access jointly adaptive to traffic and channel, in: Proc. of QoS-IP 2003, Milan, February 2003, pp. 485–498.

[3] M. Femminella, L. Piacentini, Mobility management in a reconfigurable environment: the RAMON approach, in: Proc. of QoS-IP 2003, Milan, February 2003, pp. 499–512.

[4] G. Morabito et al., Improving end-to-end performance in reconfigurable networks through dynamic setting of TCP parameters, in: Proc. of QoS-IP 2003, Milan, February 2003, pp. 513–524.

[5] H. Wang, R. Katz, J. Giese, Policy enabled handoffs across heterogeneous wireless networks, in: WMCSA 1999, New Orleans, LA.

[6] M. Inoue, K. Mahmud, H. Murakami, M. Hasegawa, MIRAI: a solution to seamless access in heterogeneous wireless networks, in: IEEE ICC 2003, Anchorage, USA.

[7] M. Buddikot, G. Chandranmenon, S. Han, Y.W. Lee, S. Miller, L. Salgarelli, Integration of 802.11 and third-generation wireless data networks, in: Infocom 2003, San Francisco, USA.

[8] E. Brewer et al., A network architecture for heterogeneous mobile computing, IEEE Personal Communications 5 (5) (1998) 8–24.

[9] A. Boulis, P. Lettieri, M. Srivastava, Active base stations and nodes for wireless networks, Wireless Networks 9 (1) (2003) 37–49.

[10] V. Bose, M. Ismert, M. Welborn, J. Guttag, Virtual radios, IEEE Journal on Selected Areas of Communications 17 (4) (1999) 591–602.

[11] A.H. Aghvami, T.h. Le, N. Olaziregi, Mode switching and QoS issues in software radio, IEEE Personal Communications 8 (5) (2001) 38–44.

[12] M.A. Beach et al., Re-configurable radio systems & networks, in: Proc. of 3G Mobile Communication Technologies, 2000.

[13] J. Brakenslek et al., Software radio approach for re-configurable multi-standard radios, in: PIMRC'02, 2002.

[14] D. Panigrahi et al., A hardware/software reconfigurable architecture for adaptive wireless image communication, in: Proc. of VLSID'02, 2002.

[15] Z. Haas, On the performance of medium access control scheme for the reconfigurable wireless networks, in: IEEE MILCOM 1997, Monterey, CA, 1997.

[16] X. Zhao, C. Castelluccia, M. Baker, Flexible network support for mobility, in: ACM/IEEE MobiCom 1998, Dallas, USA, 1998.

[17] M. Stemm, R.H. Katz, Vertical handoffs in wireless overlay networks, Mobile Networking 3 (4) (1998) 335–350.

[18] M.E. Kounavis, A.T. Campbell, G. Ito, G. Bianchi, Design, implementation and evaluation of programmable handoff in mobile networks, Mobile Networking 6 (2001) 443–461.

[19] G. Bianchi, I. Tinnirello, Improving load balancing mechanisms in wireless packet networks, in: IEEE ICC 2002, New York, USA, April 2002.

[20] A.T. Campbell et al., Comparison of IP micromobility protocols, IEEE Wireless Communications 9 (1) (2002) 72–82.

[21] C. Perkins, IP mobility support, in: RFC 2002, October 1996.

[22] D.B. Johnson, C. Perkins, Mobility support in IPv6, Internet draft, draft-ietf-mobileip-ipv6-18.txt, June 2002, work in progress.

[23] A.G. Valko, Cellular IP—a new approach to Internet host mobility, ACM Computer Communications Review 29 (1) (1999) 50–65.

[24] G. Patel, S. Dennett, The 3GPP and 3GPP2 movements towards an all-IP mobile network, IEEE Personal Communications 7 (4) (2000) 62–64.

[25] L. Bos, S. Leroy, Toward an all-IP-based UMTS system architecture, IEEE Network 15 (1) (2001) 36–45.

[26] R. Ramjee, T.F. La Porta, L. Salgarelli, S. Thuel, K. Varadhan, IP-based access network infrastructure for next-generation wireless data networks, IEEE Personal Communications 7 (4) (2000) 34–41.

[27] F.M. Chiussi, D.A. Khotmsky, S. Krishnan, Mobility management in third-generation all-IP networks, IEEE Communications Magazine 40 (9) (2002) 124–135.

[28] S. Hadjiefthymiades, S. Papayiannis, L. Merakos, Using path prediction to improve TCP performance in wireless/mobile communications, IEEE Communications Magazine 40 (8) (2002) 54–61.

[29] C.-F. Chiasserini, M. Meo, A re-configurable protocol setting to improve TCP over wireless, IEEE Transactions on Vehicular Technology 51 (6) (2002) 1608–1620.

[30] A. Baiocchi, F. Cuomo, C. Martello, Optimizing the radio resource utilization of multiaccess systems with a traffic transmission quality adaptive packet scheduling, Computer Networks 38 (2) (2002) 225–246.

[31] Network Simulator ns, UC Berkeley, LBL, USC/ISI, Xerox PARC. Internet site: http://www.isi.edu/nsnam/ns.

[32] J. Widmer, Network simulations for a mobile network architecture for vehicles, Internet site: http://www.icsi.berkeley.edu/~widmer/mnav/ns-extension/.

[33] Bluehoc simulator site: http://www-124.ibm.com/developerworks/opensource/bluehoc/.

[34] Bluetooth SIG, Specification of the Bluetooth System-Version 1.1, Specification volume I–II, February 2001.

Carla-Fabiana Chiasserini graduated with a summa cum laude degree in Electrical Engineering from the University of Florence in 1996. She did her graduate work at the Politecnico di Torino, Italy, receiving the Ph.D. degree in 1999. Since then she has been with the Department of Electrical Engineering at Politecnico di Torino, where she is currently an assistant professor. Since 1999, she has worked as a visiting researcher at the University of California, San Diego, CA.

Her research interests include architectures, protocols and performance analysis of wireless networks for integrated multi-media services.

Francesca Cuomo graduated with a summa cum laude degree in Electrical Engineering in 1993, from the University of Rome ''La Sapienza,'' Italy. She earned the Ph.D. degree in Information and Communications Engineering in 1998, also from the University of Rome ''La Sapienza''. Since 1996 she is a researcher at the INFOCOM Department of this University.

Her main research interests focus on modeling and control of broadband integrated networks, signaling and intelligent networks, architectures and protocol for fixed an mobile wireless networks, mobile and personal communications, quality of service guarantees and real time service support in the Internet and in the radio access, reconfigurable radio systems and wireless ad hoc networks.

She participated in (I) the European ACTS INSIGNIA project dedicated to the definition of an Integrated IN and B-ISDN network; (II) RAMON project, funded by the Italian Public Education Ministry; (III) National project ''Multimedialità'' CNR-MURST. She is now participating to the European IST WHYLESS.COM project focusing on adoption of the Ultra Wide Band radio technology for the definition of an Open Mobile Access Network. In this project she is leader of the WP4 (Network Resource Manager). As for current national projects (I) she is involved in FIRB project VIRTUAL IMMERSIVE COMMUNICATIONS (VICOM) where she is responsible of the research activities on the BAN and VAN networks; (II) she is responsible of the research unit at the University of Rome ''La Sapienza'' in the EURO project funded by the Italian Public Education Ministry.

Leonardo Piacentini graduated with a summa cum laude degree in Electrical Engineering from the University of Perugia in 2001. Since January 2002, he has been working as a Ph.D. student of the Department of Electronic and Information Engineering (DIEI) at the University of Perugia.

His actual research is focusing on mobility in wireless networks. He has been involved in the projects RAMON, VICOM, PRIMO, co-funded by the Italian Ministry for Education, Higher Education and Research (MIUR).

Michele Rossi graduated with a summa cum laude degree in Electrical Engineering from the University of Ferrara in 2000, where he currently is pursuing the Ph.D. degree. In 2000–2001 he was a research fellow at the Department of Engineering, University of Ferrara. From April 2003 to October 2003 he has been doing research at the Center for Wireless Communications (CWC) at the University of California, San Diego, USA.

His research interests are on TCP/IP protocols on wireless networks, TCP/IP header compression, performance analysis of link layer retransmission techniques, efficient multi-cast data delivery and mobility in 3G cellular networks.

Ilenia Tinnirello graduated with a summa cum laude degree in Electrical Engineering from the University of Palermo, Italy, in 2000. Since November 2000, she has been a Ph.D. student in Telecommunications at University of Palermo.

Her main interests are resource management schemes in wireless networks and ad hoc network MAC protocols.

Francesco Vacirca graduated in Telecommunications Engineering from the University of Rome "La Sapienza", Italy, in 2001. From September 2001 to December 2002 he participated to the RAMON project, working on reconfigurable wireless systems. He is currently a Ph.D. student of Prof. Andrea Baiocchi at the Infocom Department of the University of Rome "La Sapienza".

His research focuses on wireless network optimization for mobile computing applications.